# Inelastic scattering of 66.5 MeV protons from $^{148}$Sm and $^{154}$Sm

A. Guterman,* D. L. Hendrie,† P. H. Debenham,‡ K. Kwiatkowski,§ A. Nadasen,** and L. W. Woo§
*University of Maryland, College Park, Maryland 20742*

R. M. Ronningen
*National Superconducting Cyclotron Laboratory, Michigan State University, East Lansing, Michigan 48824*
(Received 12 December 1988)

Differential cross sections for the inelastic scattering of 66.5 MeV protons from $^{148}$Sm and $^{154}$Sm were measured over an angular range 8°–90° (c.m.). For $^{148}$Sm, data were obtained for the ground and the first excited states. Using the first-order vibrational model, coupled-channel calculations reproduce both states rather well. Data for the $J^{\pi}=0^{+}-6^{+}$ members of the roatational band of $^{154}$Sm were also obtained. $^{154}$Sm was treated as a rigid rotor and coupled-channel calculations were carried out in terms of the deformation of the $^{148}$Sm spherical optical-model potential. Deformation parameters $\beta_2$, $\beta_4$, and $\beta_6$ have been extracted. Contrary to results of $(\alpha,\alpha')$scattering at 50 MeV and proton inelastic scattering at 800 MeV, the data show preference for a positive value of $\beta_6$, in agreement with $(p,p')$ studies at 35 and 135 MeV and the calculations of Nilsson *et al.*

## I. INTRODUCTION

Studies of the collective properties of permanently deformed nuclei by hadronic scattering in many cases employ phenomenological approaches, because of limited understanding of the effective nucleon-nucleon interaction in the environment of nuclear matter. For example, the analysis of proton scattering data typically begins with a parametrized phenomenological optical-model potential to describe scattering from the ground state. Then, an analysis of excited-state data proceeds by deforming the potential and solving coupled-channel equations. The parameters of the deformed optical-model potential (DOMP) characterize the collectivity and can be related to fundamental nuclear properties such as the shape or the matter distribution.

In the analysis of the $^{148,154}$Sm$(\alpha,\alpha')$ data at 50 MeV,[1] an optical-model potential was first determined with the elastic scattering data for the spherical $^{148}$Sm nucleus. Since this potential is inherently independent of shape and should vary smoothly for a wide range of nuclei, it was argued that the same potential could be used for the deformed $^{154}$Sm, with modifications only to account for its shape. Thus, the excitations of rotational states in the deformed $^{154}$Sm nucleus were described by introducing deformation parameters into the optical-model potential obtained for the spherical $^{148}$Sm nucleus. The deformation parameters contain information on the nuclear shape. We report here the evaluation of this procedure for the $(p,p')$ reactions at 66.5 MeV on the same nuclei.

An important advantage of the $(p,p')$ reactions at 66.5 MeV is that the $4^{+}$ and $6^{+}$ members of the ground-state rotational band are rather strongly excited. Information on deformations of order higher than quadrupole should be contained in these data. One may extract shape information from the DOMP using a theorem due to Satchler.[2] Mackintosh has pointed out that, to the extent that the DOMP can be derived from a folding model in which the proton and neutron distributions are the same and the folding interaction is local and energy independent, the properly normalized multipole moments of the DOMP are equal to those of the matter distribution.[3] The crucial assumption is about the nature of the interaction. Ichihara *et al.*[4] used polarized proton scattering on heavier rare-earth nuclei at nearly the same energy as our study. They found it necessary to include density dependence in the effective interaction to reconcile the difference (about five percent for quadrupole moments) between moments deduced from the DOMP used in their study and moments deduced from electron scattering or Coulomb excitation measurements where the interactions are known. Brieva and Giorgiev[5] have further predicted an energy dependence in the multipole moments derived from the DOMP, reflecting the energy dependence of the effective interaction.

The nucleus $^{154}$Sm is useful for studying the above facets because it is well deformed and many experiments using hadronic and electromagnetic probes at several energies have been carried out on it. Most generally agree on quadrupole and hexadecapole moments within the uncertainties of measurement and analysis. Proton scattering even at an energy as low as 35 MeV is sensitive to the hexacontatetrapole moment, whose first-order term contains the $\beta_6$ deformation parameter.[5] The $\beta_6$ extracted from proton scattering experiments at 35 (Ref. 6) and 134 MeV (Ref. 7) is positive, while studies of $(\alpha,\alpha')$ at 50 MeV (Ref. 1) and $(p,p')$ at 800 MeV (Ref. 8) have provided a negative value. We show here agreement with the former studies and with theoretical calculations by Nilsson *et al.*[9]

## II. EXPERIMENT

The experiment was performed using a 66.5 MeV proton beam from the University of Maryland Sectored Isochronous Cyclotron. In order to reduce beam-related

 

background the beam was sent through two 90° bending magnets and a beam energy analyzing magnet. This provided a clean beam with an energy resolution $\leq 25$ keV and angular divergence $\leq 0.5°$.

The beam was focused onto targets placed at the center of a 43-cm-diam scattering chamber. The beam spot on target was generally 1 mm wide by 2 mm high. The targets used were self-supporting $2.4\pm0.1$-mg/cm$^2$ $^{148}$Sm (96.4% isotopically pure) and $3.25\pm0.1$-mg/cm$^2$ $^{154}$Sm (98.7% isotopically pure).

The scattered particles were detected with a QDS magnetic spectrometer consisting of an entrance quadrupole, an $n=\frac{1}{2}$, 180°, dipole, and an exit sextupole. The entrance slits to the spectrometer subtended an angle of 0.95°. The first element of the focal-plane detection system was a 0.5-mm-deep position-sensitive Si detector (PSD). The dimensions of the PSD were 8 mm high and 5 cm wide. A 7.6-mm-high slit was placed in front of it in order to eliminate edge effects. By rotating the detector about a vertical axis relative to the focal plane it was determined that a detector angle of 50° provided optimum resolution with an energy bite of approximately 800 keV, which was sufficient for the present experiment. It was followed by two plastic scintillators, one 6.35 mm deep and the other 12.7 mm deep. The plastic scintillators, serving as $\Delta E$ detectors, provided particle identification (PID).

In a two-dimensional display of the signals from the plastic scintillators, protons were cleanly separated from other particles arriving at the focal plan. A window around the protons in the PID spectrum was used to gate the PSD spectrum, resulting in an energy spectrum of protons. With each setting of the dipole, the quadrupole and sextupole were also adjusted to optimize the energy resolution. The resulting energy resolution ranged between 25 and 50 keV.

A 5-mm Si(Li) detector was used as a monitor. This monitor was placed downstream from the target at an angle of 24° with the beam for large-angle measurements, and at −38° for measurements at small angles. A counter-bored water-cooled Faraday cup was used for charge collection of the beam particles. It subtended an angle of 5°. Consistency between the monitor counts and the integrated charge of the Faraday cup provided confidence in the stability of the beam. Pulses generated at a rate proportional to the beam current were fed to the focal-plane detection system and processed together with the real events in order to determine the dead time of the data acquisition system.

One- and two-dimensional arrays of the data created during the experiment served to monitor dead-time, pile-up, energy resolution, and changes in experimental conditions. Measurements were made from 7.5° to 90° (in the laboratory) in angular steps of 2.5° for both targets. All data were written to magnetic tapes for later off-line analysis.

## III. EXPERIMENTAL RESULTS

During replay of the $^{148}$Sm runs, the areas under the ground state ($0^+$), the 550-keV state ($2^+$), and the pulser

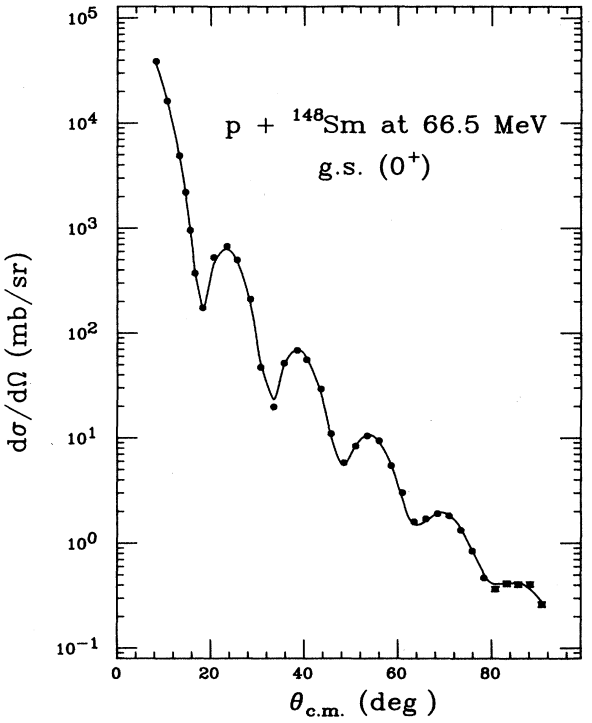


FIG. 1. Angular distribution of the differential cross sections for the elastic scattering of 66.5 MeV protons from $^{148}$Sm. The curve represents coupled-channels calculations using the first-order vibrational model.

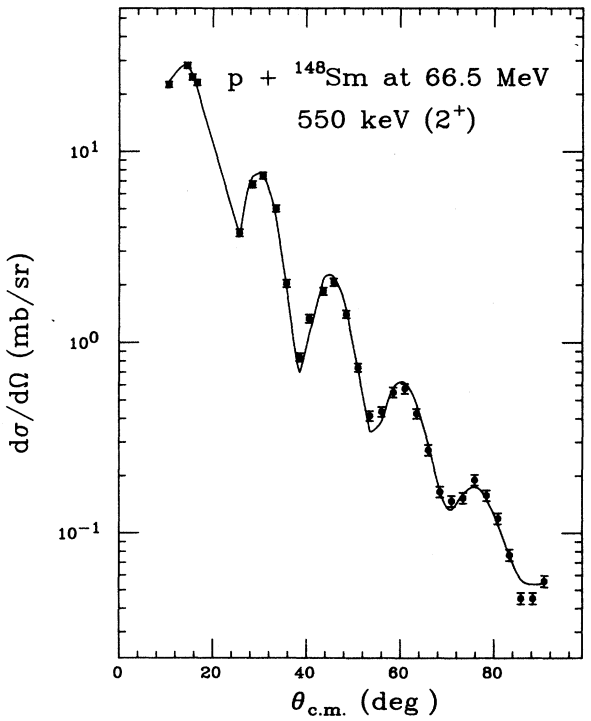


FIG. 2. Differential cross sections for the inelastic scattering of 66.5 MeV protons to the first excited state of $^{148}$Sm. The curve represents coupled-channels calculations using the first-order vibrational model.

peak were extracted. A constant background was assumed for each peak. The value of the background was determined by the counts on either side of the peak. Cross sections were then calculated for the two states. For $^{154}$Sm, the ground state ($0^+$) and the 82-keV state ($2^+$) were resolved. However, because of the overlap of the tails of the peaks, a peak-fitting technique was used to derive a separate cross section for exact state. The $4^+$, $6^+$, and pulser peaks were extracted by assuming a constant background. The pulser counts were used to correct the data for dead time.

To ensure that counts were not missed by the PSD because of its limited height, cross sections were compared with earlier measurements using a large low-resolution single-wire proportional counter. For states that could be resolved by the gas counter, the two measurements agreed within statistics. This comparison confirmed that the efficiency of the PSD was as good as the gas counter and that data obtained with it would be reliable.

Figures 1 and 2 show the data obtained for $^{148}$Sm. The ground state ($0^+$) cross sections extend over 5 orders of magnitude in going from 8° to 90° (c.m.). The 550-keV ($2^+$) data were obtained from 9° to 90° and cross sections below 50 $\mu$b/sr were measured. For $^{154}$Sm, cross sections for $0^+$, $2^+$, $4^+$, and $6^+$ were obtained. These are shown in Figs. 3–6. The elastic scattering data covered almost 6 orders of magnitude. The lowest cross section of 10 $\mu$b/sr was obtained for the $6^+$ state.

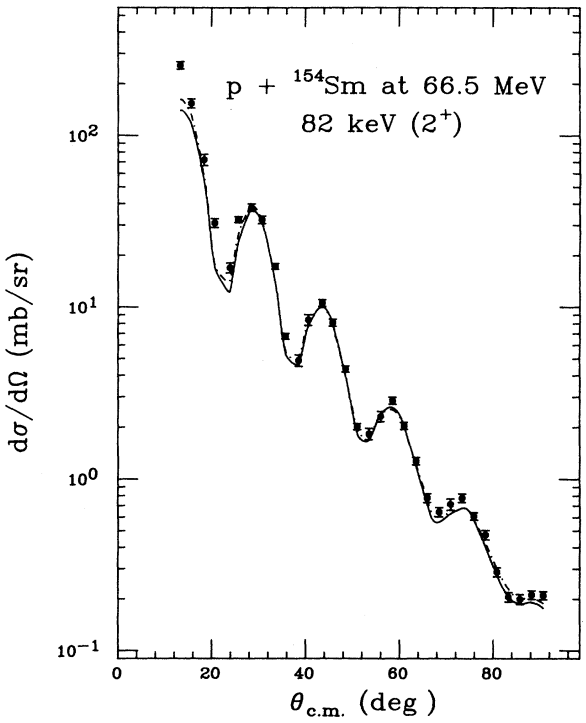


FIG. 4. Same as Fig. 3 but for the $2^+$ state of $^{154}$Sm.

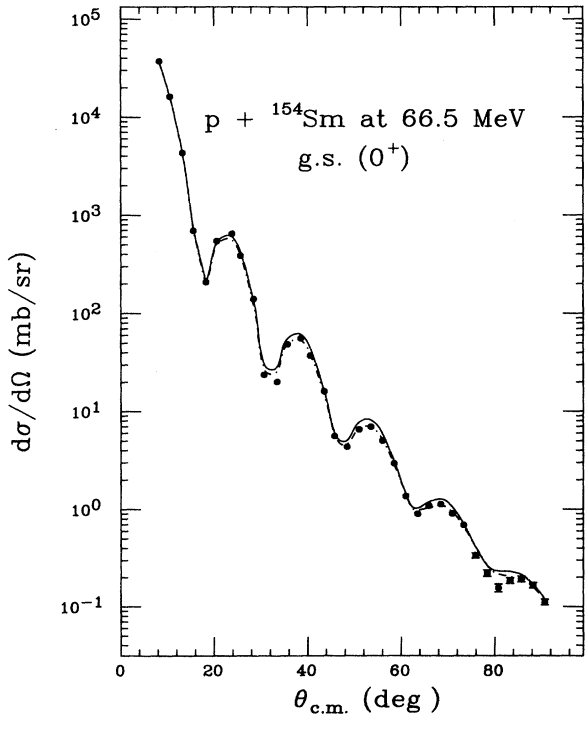


FIG. 3. Angular distribution of the differential cross sections for the elastic scattering of 66.5 MeV protons from $^{154}$Sm. The solid curve represents coupled-channels calculations with deformation of the $^{148}$Sm spherical potentials. The dot-dashed curve is the result of searching on all parameters, except the radii.

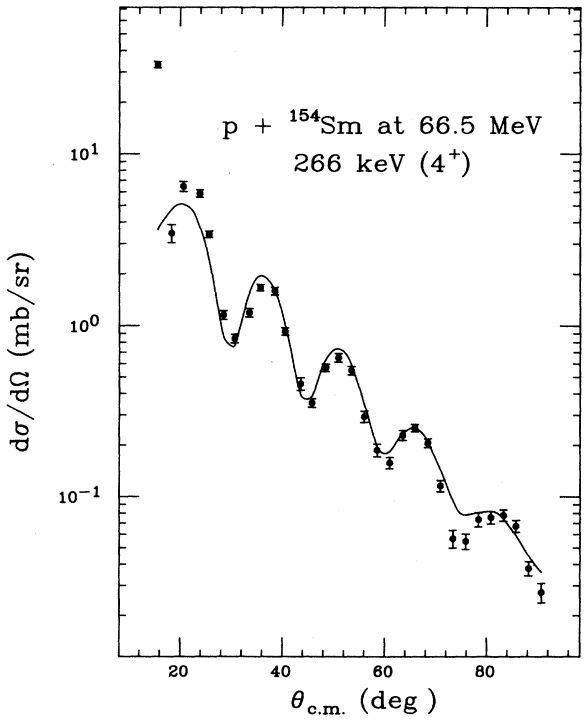


FIG. 5. Differential cross sections for the inelastic scattering of 66.5 MeV protons to the $4^+$ state of $^{154}$Sm. The curve represents coupled-channels calculations with deformation of the $^{148}$Sm spherical potentials.

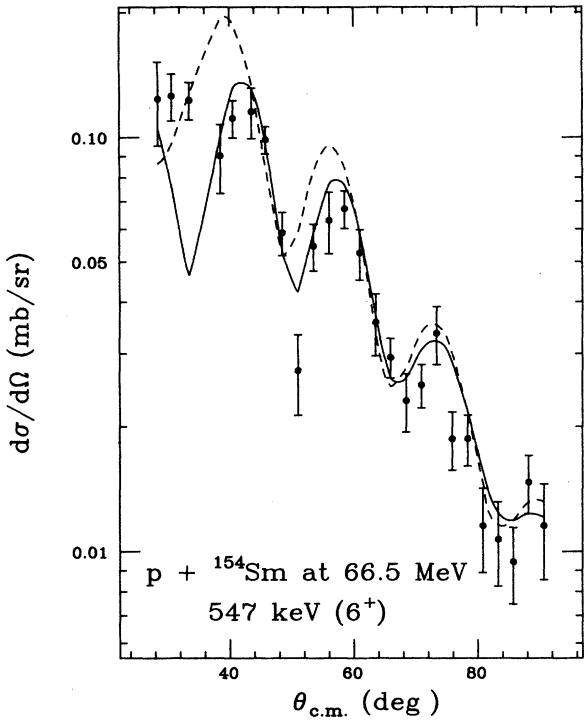


FIG. 6. Differential cross sections for the inelastic scattering 66.5 MeV protons to the $6^+$ state of $^{154}$Sm. The solid curve represents coupled-channels calculations with deformation of the $^{148}$Sm spherical potentials and a positive $\beta_6$. The dashed curve represents calculations with a negative $\beta_6$.

During error analysis it was determined that, excluding statistics, there was about 3% uncertainty inherent in each measurement. This was attributed to such factors as target nonuniformity, dead times, changes in beam direction and beam position on target, and uncertainties in charge collection efficiency of the Faraday cup. Repeated measurements seem to concur with this result. Therefore, the relative error for each datum point was obtained by adding a 3% uncertainty quadratically with the statistical uncertainty. These are indicated in Figs. 1–6, where the errors exceed the size of the data points. The absolute uncertainties in the data were estimated to be between 5% and 10%.

## IV. DATA ANALYSIS

The angular distributions of cross sections were analyzed in the standard manner using a DOMP to determine the transition matrix elements. Most of the calculations were carried out using the coupled-channels code ECIS79.[10] However, to obtain starting values, the code JIB (Ref. 11) was used to analyze the $^{148}$Sm elastic scattering data. The potentials used were of the Woods-Saxon form, consisting of real central, volume and surface absorption, and complex spin-orbit terms. Using ECIS79 and its automatic search routine, the parameters $V$, $W$, $W_d$, $V_{SO}$, $W_{SO}$, $a_R$, $a_I$, $a_{SO}$, $\beta_2^R$, $\beta_2^I$, and $\beta_2^{SO}$ were adjusted to fit both the elastic and inelastic scattering data. The radius parameters were kept fixed at the values found from the JIB calculations. In these calculations, $^{148}$Sm was assumed to be a vibrational nucleus and the first-order vibrational model was used to couple the ground state to the first $2^+$ state. The calculations are shown as solid lines in Figs. 1 and 2 and the resulting parameters are listed in Table I. The $\beta_2$ and $\chi^2$ values are given in Table II.

The standard optical-model potential determined for $^{148}$Sm (that is, given by the set of parameters in Table I), excluding deformations, was used as the "spherical" part of the DOMP for $^{154}$Sm, which was treated as a rigid rotor. All nonzero couplings to order 12 involving the ground-state rotational band through the $8^+$ state and deformations $\beta_2$, $\beta_4$, and $\beta_6$ were included. The same value of $\beta_6$ was used for every nuclear potential. To further simplify the calculations, the $\beta_2$ and $\beta_4$ values for the real-central and both spin-orbit potentials were kept the same but allowed to be different from those of the imaginary potentials in order not to constrain the $\beta R$ values on account of differences in geometry. It should be noted that the radii of the spin-orbit and real-central potentials are nearly the same but smaller than those of the imaginary volume and surface potentials.

In the initial coupled-channels calculations for $^{154}$Sm only the deformation parameters were allowed to vary, while the spherical part of the potential determined for $^{148}$Sm was kept the same. The results are shown as solid lines in Figs. 3–6. Indeed, the quality of the fits shows that the scattering of protons from a deformed nucleus can be described by the deformation of a spherical potential, or equivalently, that the optical-model potential can consist of a part which varies smoothly with mass and one which contains the strong couplings.[1] The parameters of the DOMP are given in Tables I and II (set A) along with the reduced $\chi^2$ values for each angular distribution.

In an attempt to obtain better fits, the next calculation allowed the optical-model parameters to vary along with the deformation parameters. While some improvements were noted for the ground and first excited states as

TABLE I. Best fit optical-model parameters. The radii were kept fixed in the searches. The Coulomb potential radius and diffuseness were fixed at 1.1 and 0.6 fm.

| Nucleus | $V$ (MeV) | $r_R$ (fm) | $a_R$ (fm) | $W$ (MeV) | $W_d$ (MeV) | $r_I$ (fm) | $a_I$ (fm) | $V_{SO}$ (MeV) | $W_{SO}$ (MeV) | $r_{SO}$ (fm) | $a_{SO}$ (fm) |
|---|---|---|---|---|---|---|---|---|---|---|---|
| $^{148}$Sm | 35.62 | 1.24 | 0.657 | 4.73 | 2.83 | 1.38 | 0.655 | 4.90 | −0.15 | 1.23 | 0.840 |
| $^{154}$Sm (set A) | 35.62 | 1.24 | 0.657 | 4.73 | 2.83 | 1.38 | 0.655 | 4.90 | −0.15 | 1.23 | 0.840 |
| $^{154}$Sm (set B) | 34.71 | 1.24 | 0.707 | 2.43 | 3.37 | 1.38 | 0.801 | 3.68 | −0.57 | 1.23 | 0.830 |
| $^{154}$Sm (set C) | 34.65 | 1.24 | 0.718 | 3.23 | 2.71 | 1.38 | 0.811 | 3.56 | −0.75 | 1.23 | 0.830 |

TABLE II. Best fit deformation parameters and reduced chi-squared values. The Coulomb potential deformation parameters were kept fixed in all searches. For $^{148}$Sm, $\beta_2^C$ was chosen so that with the radius and diffuseness values given in Table I, the adopted $B(E2)$ value from the compilation of Raman *et al.* (Ref. 12) is obtained. For $^{154}$Sm, the $\beta_2^C$ and $\beta_4^C$ values were chosen so as to obtain the error-weighted-average values of the $E2$ and $E4$ matrix elements in the survey by Ronningen *et al.* (Ref. 7).

| Nucleus | $\beta_2^{R,SO}$ | $\beta_4^{R,SO}$ | $\beta_6$ | $\beta_2^I$ | $\beta_4^I$ | $\chi^2_{0^+}$ | $\chi^2_{2^+}$ | $\chi^2_{4^+}$ | $\chi^2_{6^+}$ |
|---|---|---|---|---|---|---|---|---|---|
| $^{148}$Sm | 0.119 | | | 0.172 | | 4.7 | 3.73 | | |
| $^{154}$Sm (set A) | 0.247 | 0.066 | 0.007 | 0.253 | 0.054 | 13.8 | 10.2 | 23.9 | 3.4 |
| $^{154}$Sm (set B) | 0.258 | 0.061(4) | 0.006(4) | 0.235(4) | 0.069(19) | 6.6 | 6.3 | 23.8 | 3.2 |
| $^{154}$Sm (set C) | 0.260 | 0.061 | −0.006 | 0.235 | 0.069 | 6.5 | 5.3 | 21.9 | 7.2 |

shown by the dot-dashed curves in Figs. 3 and 4, fits for the $4^+$ and $6^+$ states were essentially the same. The deformation parameters from the second calculation are very similar to those from the first calculation. The resulting parameters and reduced $\chi^2$ values are also given in Tables I and II (set B). The uncertainties shown in Table II, set B, are statistical and come from the searching procedure in ECIS79.

The above analysis favors a positive value for $\beta_6$. This result is somewhat surprising in view of the $(\alpha,\alpha')$ scattering study at 50 MeV (Ref. 1) and $(p,p')$ study at 800 MeV.[8] However, it is in agreement with $(p,p')$ studies at 35 (Ref. 6) and 135 MeV.[7] To test the uniqueness of the positive value of $\beta_6$ two more calculations were done. In the first, we simply reversed the sign of $\beta_6$ keeping all other parameters from the aforementioned search fixed. Second, a search was made on all parameters with the negative value of $\beta_6$ left fixed. The resulting parameters are listed in Tables I and II (set C). While the total $\chi^2$ of all the states for either sign of $\beta_6$ are comparable, the $\chi^2$ of the $6^+$ level is about twice that obtained for a positive value of $\beta_6$. The calculated cross sections are shown as dashed lines in Fig. 6. It is clear that the calculations give a poorer fit for angles forward of 60°. Including the negative $\beta_6$ in the search resulted in no significant improvement to the fits. Therefore, it may be reasonable to assume that our investigations show support for the calculations by Nilsson *et al.*,[9] which indicate that $\beta_6$ may be positive in both the light rare-earth and heavy transition-metal regions and negative in the middle of the rare-earth region.

In Table III we list the multipole moments for $^{154}$Sm derived from proton scattering at different energies. It is observed that there is excellent agreement for the quadrupole and hexadecapole moments obtained from the various studies. However, the hexacontatetrapole moment derived at 800 MeV is smaller than those from the lower-energy investigations, a reflection of the negative $\beta_6$ value they use in their analysis.

## V. SUMMARY AND CONCLUSIONS

We have measured the differential cross sections for the elastic and inelastic scattering of 66.5 MeV protons from $^{148}$Sm and $^{154}$Sm. Angular distributions extending up to 90° were obtained for the ground $(0^+)$ and 550 keV$(2^+)$ states of $^{148}$Sm and for the $0^+$, $2^+$, $4^+$, and $6^+$ states of the ground-state rotational band of $^{154}$Sm. The data show reasonably strong excitations of the high-spin states.

Analysis in the framework of a first-order vibrational model reproduces the $^{148}$Sm data reasonably well. $^{154}$Sm was treated as a rigid rotor and the analysis indicates that it is feasible to describe the data in terms of the deformation of a spherical optical-model potential generated from the $^{148}$Sm data. The derived deformation parameters are in agreement with previous studies, except for the sign of $\beta_6$. Acceptable fits to the data are obtained for the first three levels with either sign for $\beta_6$. However, an improved fit is obtained for the $6^+$ level with a positive value of $\beta_6$. The predictions of Nilsson *et al.* of a positive $\beta_6$ is supported by $(p,p')$ studies at 35 and 134 MeV. However, a negative value for $\beta_6$ is derived from the analyses of alpha inelastic scattering at 50 MeV and proton

TABLE III. Moments of the DOMP obtained in this work together with other results.

| Reaction | Energy (MeV) | $q_{20}$ ($eb$) | $q_{40}$ ($eb^2$) | $q_{60}$ ($eb^3$) | Reference |
|---|---|---|---|---|---|
| $(p,p')$ | 35[a] | 2.06(3) | 0.54(2) | | King *et al.*, Ref. 6 |
| $(p,p')$ | 35[b] | 1.99 | 0.51 | 0.13 | Ronningen *et al.*, Ref. 13 |
| $(p,p')$ | 66.5 | 2.16(5) | 0.57(4) | 0.15(3) | This work |
| $(p,p')$ | 135 | 2.31(8) | 0.62(6) | 0.19(4) | Ronningen *et al.*, Ref. 7 |
| $(p,p')$ | 800[c] | 2.12 | 0.58 | 0.099 | Barlett *et al.*, Ref. 8 |
| $(p,p')$ | 800[d] | 2.12 | 0.54 | 0.088 | Ray, Ref. 14 |
| Coulomb excitation | | 2.094(4) | 0.588(29) | | See Ronningen *et al.*, Ref. 7 |

[a] $\beta_6$ not included in the analysis.
[b] Data set of footnote a, extended and $\beta_6$ included.
[c] No spin-orbit interaction.
[d] Same data as in footnote c but the spin-orbit interaction was included in the analysis.

inelastic scattering at 800 MeV.

In view of the differences in the sign of $\beta_6$ obtained from the different experiments, it is reasonable to ask whether this could be an artifact of different methodologies of analysis. However, it has to be noted that analyses of all the proton scattering data (Refs. 6, 7, 14, and this work) have been carried out with the code ECIS79 with its standard features. Therefore, it is unlikely that the discrepancy could be attributed to different types of calculations. Nevertheless, it has to be pointed out the fit to the $6^+$ data in the lower-energy analyses is superior to that of the 800 MeV calculations[8,14] (for example, Fig. 6 of the present study can be compared with Fig. 3 of Ref. 8). Also, it appears that a search with a positive value of $\beta_6$ was not attempted in the analysis of the 50 MeV $(\alpha,\alpha')$ data.[1]

It is not clear that the present investigation has resolved this problem, although our results seem to show a preference for a positive value of $\beta_6$. Further investigations would be necessary to unambiguously answer this question.

## ACKNOWLEDGMENTS

The authors are grateful to the University of Maryland Computer Science Center and the National Superconducting Cyclotron Laboratory for their generous allocation of computer time. This work was supported in part by the National Science Foundation and the Department of Energy.

---

*Present address: Tel Aviv University, Tel Aviv 69978, Israel.
†Present address: Department of Energy, Washington, D.C. 20545.
‡Present address: National Institute of Standards & Technology, Gaithersburg, MD 20899.
§Present address: Indiana University Cyclotron Facility, Bloomington, IN 47408.
**Present address: University of Michigan, Dearborn, MI 48128.

[1]D. L. Hendrie *et al.*, Phys. Lett. **26B**, 127 (1968).
[2]G. R. Satchler, J. Math. Phys. **13**, 1118 (1972).
[3]R. S. Mackintosh, Nucl. Phys. **A266**, 279 (1976).
[4]T. Ichihara *et al.*, Phys. Rev. C **29**, 1228 (1984).
[5]F. A. Brieva and B. Z. Georgiev, Nucl. Phys. **A302**, 27 (1978).
[6]C. H. King, J. E. Finck, G. M. Crawley, J. A. Nolen, Jr., and R. M. Ronningen, Phys. Rev. C **20**, 2084 (1979); C. H. King, G. M. Crawley, J. A. Nolen Jr., and J. E. Finck, J. Phys. Soc. Jpn. Suppl. **44**, 564 (1978)
[7]R. M. Ronningen *et al.*, Phys. Rev. C **28**, 123 (1983).
[8]M. L. Barlett *et al.*, Phys. Rev. C **22**, 1168 (1980).
[9]S. G. Nilsson *et al.*, Nucl. Phys. **A131**, 1 (1969)
[10]J. Raynal, computer code ECIS79, CEN-Saclay, 1979 (unpublished).
[11]F. G. Perey (private communication).
[12]S. Raman *et al.*, At. Data Nucl. Data Tables **36**, 2 (1987).
[13]R. M. Ronningen *et al.* (unpublished).
[14]L. Ray, Phys. Lett. **102B**, 88 (1981).